# Supporting Information

## In situ Decorated $Cu_2FeSnS_4$ Nanosheet Arrays for Low Voltage Hydrogen Production through Ammonia Oxidation Reaction

Yoongu Lim,[†a] Subramani Surendran,[†a] Won So,[b] Sathyanarayanan Shanmugapriya,[a] Chanmin Jo,[a] Gnanaprakasam Janani,[a] Hyeonuk Choi,[c] Hyun Soo Han,[d] Heechae Choi,[e] Young-Hoon Yun,[f] Tae-Hoon Kim,[g] Myeong-Jin Kim,[h] Kyoungsuk Jin,[i] Jung Kyu Kim,*[,b] and Uk Sim,*[,a,j,k]

[a] *Hydrogen Energy Technology Laboratory, Korea Institute of Energy Technology (KENTECH), Naju, Jeonnam 58330, Republic of Korea. E-mail: usim@kentech.ac.kr (U. Sim)*

[b] *School of Chemical Engineering, Sungkyunkwan University, 2066 Seobu-ro, Jangan-gu, Suwon, 16419, Republic of Korea. Email: legkim@skku.edu (J. K. Kim)*

[c] *Department of Materials Science and Engineering, Korea Advanced Institute of Science and Technology, 291 Daehak-ro, Yuseong-gu, Daejeon 34141, Republic of Korea*

[d] *Department of Mechanical Engineering, Stanford University, Stanford, CA 94305, USA*

[e] *Department of Chemistry, Xi'an Jiaotong-Liverpool University, Suzhou, 215123, China*

[f] *Department of New & Renewable Energy, Dongshin University, Jeonnam 520-714, Republic of Korea*

[g] *Department of Materials Science and Engineering, Chonnam National University, Gwangju, 61186, Republic of Korea*

[h] *Department of Hydrogen & Renewable Energy, Kyungpook National University, Daegu, 41566, Republic of Korea*

[i] *Department of Chemistry, Korea University, Seoul, 02841 Republic of Korea*

[j] *Research Institute, NEEL Sciences, INC., Naju, Republic of Korea.*

[k] *Center for Energy Storage System, Chonnam National University, Gwangju, Republic of Korea.*

[†] *These authors contributed equally to this work.*

**Electrochemical measurements**

Electrochemical characterization of the CFTS nanosheets was carried out using potentiostat equipment (Bio-Logic SP150 instrumentation) at room temperature in a three-electrode cell configuration where the synthesized active material was used as the working electrode. The platinum (Pt) wire and Hg/HgO electrode were used as counter and reference electrodes. 1 M KOH solution with and without 0.5 M $NH_4OH$ was used as electrolytes to investigate the AOR activity. As the electrochemical data was measured with Hg/HgO reference electrode, the potential range was calibrated to the reversible hydrogen electrode (RHE) potential standard with $E^0_{(Hg/HgO)}$ = 118 mV using the following equation.

$$E_{RHE} = E_{(Hg/HgO)} + E^0{}_{Hg/HgO} + 0.059 \times pH$$

Electrochemical impedance spectroscopy measurements were conducted, and Bode plots were obtained in the frequency range of ~0.1–105 Hz at 0 V vs. Hg/HgO. A flow-type lab-scale water electrolyzer setup was performed with 1 M KOH and 1 M KOH with 0.5 M $NH_4OH$ electrolyte as catholyte and anolyte, respectively. The electrodes are separated using a Nafion membrane. The catholyte and anolyte are fed into the respective chambers by a separate peristaltic pump which carries the resultant product after electrolysis. The obtained $H_2$ gas is collected in an air-tight receptacle and measured with a gas $H_2$ gas detector.

**The calculation of Turnover frequency (TOF)**

TOF of catalyst: The number of oxygen turnovers was calculated from the current density using the following equation,

TOF = j *Ag / 4* F* n

where j is the measured current density at 1.8, 1.9, 2.0, 2.1, and 2.2 V, respectively; Ag is the surface area of the electrode; F is the Faraday constant (96485.3 C $mol^{-1}$); and n is the moles of the catalyst loaded on the electrode.

**The calculation of Faradaic efficiency**

The electrocatalytic water splitting experiment was conducted in a two-electrode system, with EG-CFTS (1 cm × 1cm) as the cathode and anode.

The Faradaic efficiency is calculated by FE(%) = $n_{exp}/n_{Theo}$,

Where $n_{exp}$ means the total number of moles of the collected $H_2$ and $O_2$ gases and

nTheo = 3Q/(4F) (Q is the charge passing through the electrodes, and F is Faraday constant).

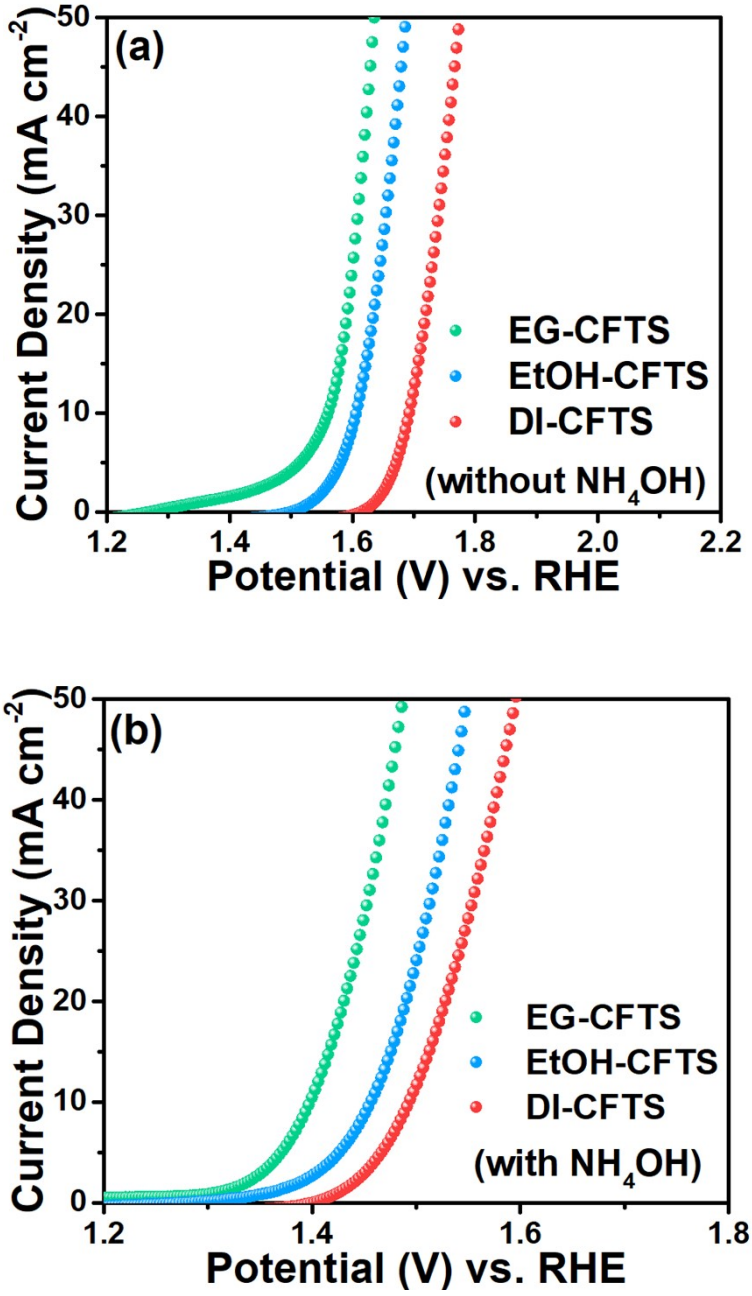


**Fig. S1** Magnified images of (a) OER and (b) AOR LSV polarization curves depicting the overpotential at 10 mA $cm^{-2}$, respectively.

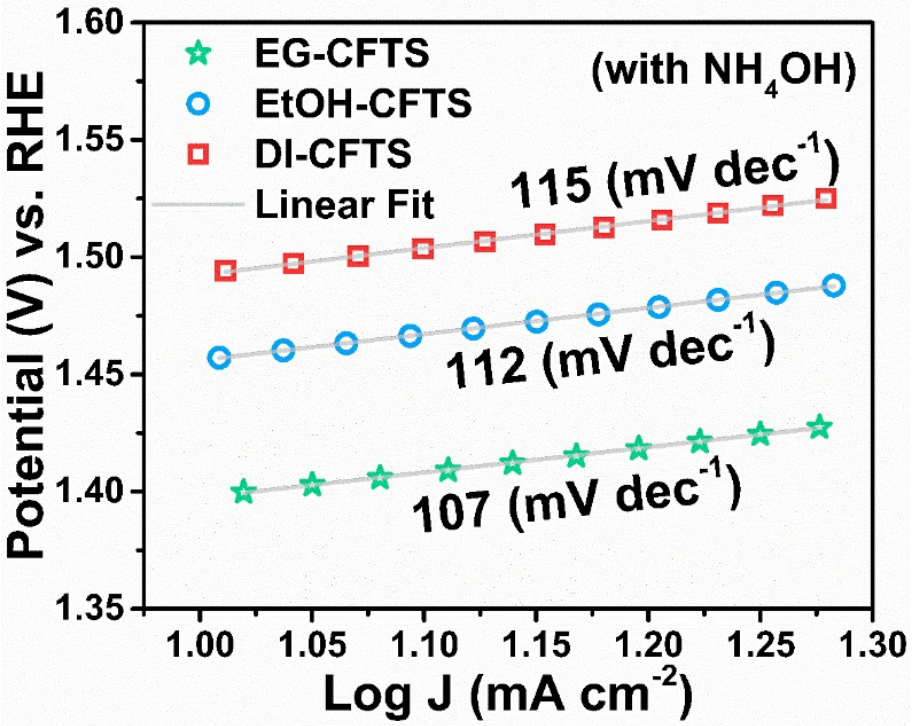


**Fig. S2** Tafel plot for the prepared CFTS electrocatalysts.

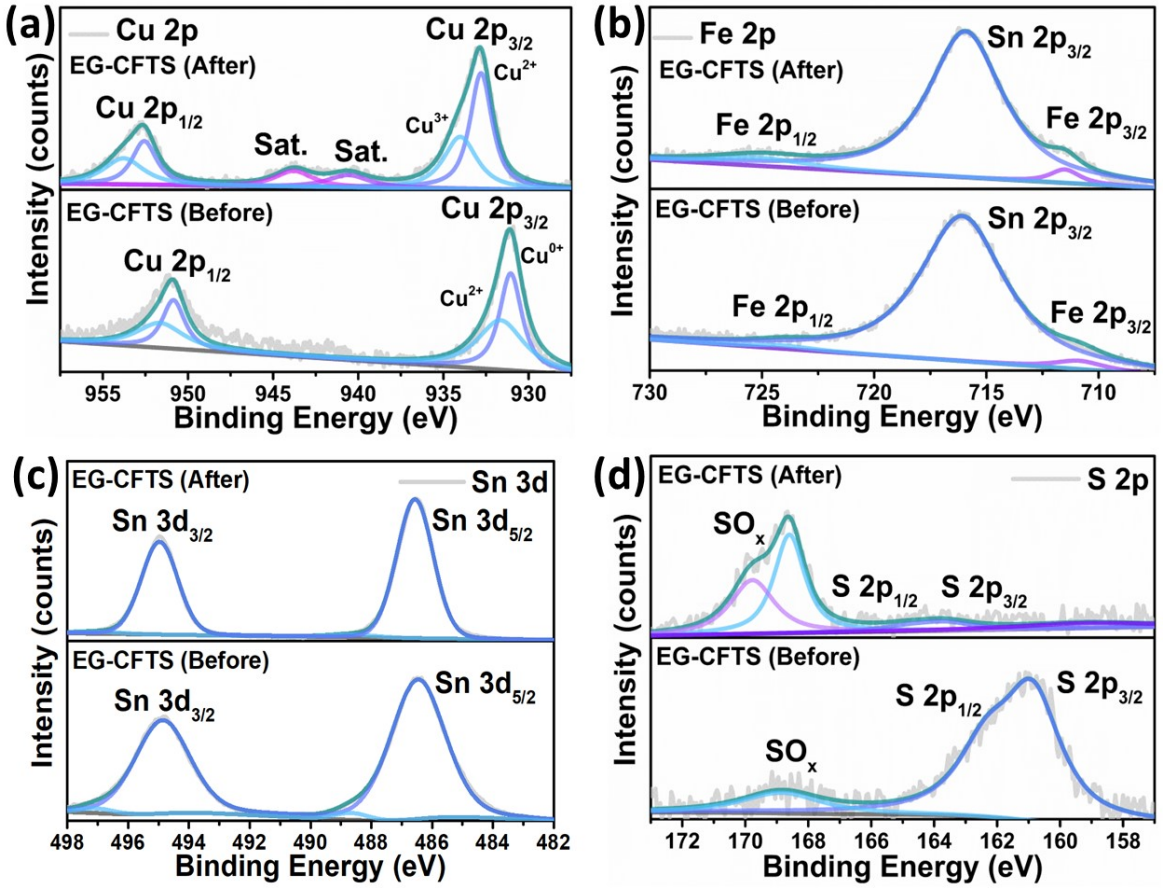


**Fig. S3** High-resolution XPS spectra for EG-CFTS samples before and after electrochemical tests: a) Cu 2p, b) Fe 2p, c) Sn 3d, and d) S 2p, respectively.

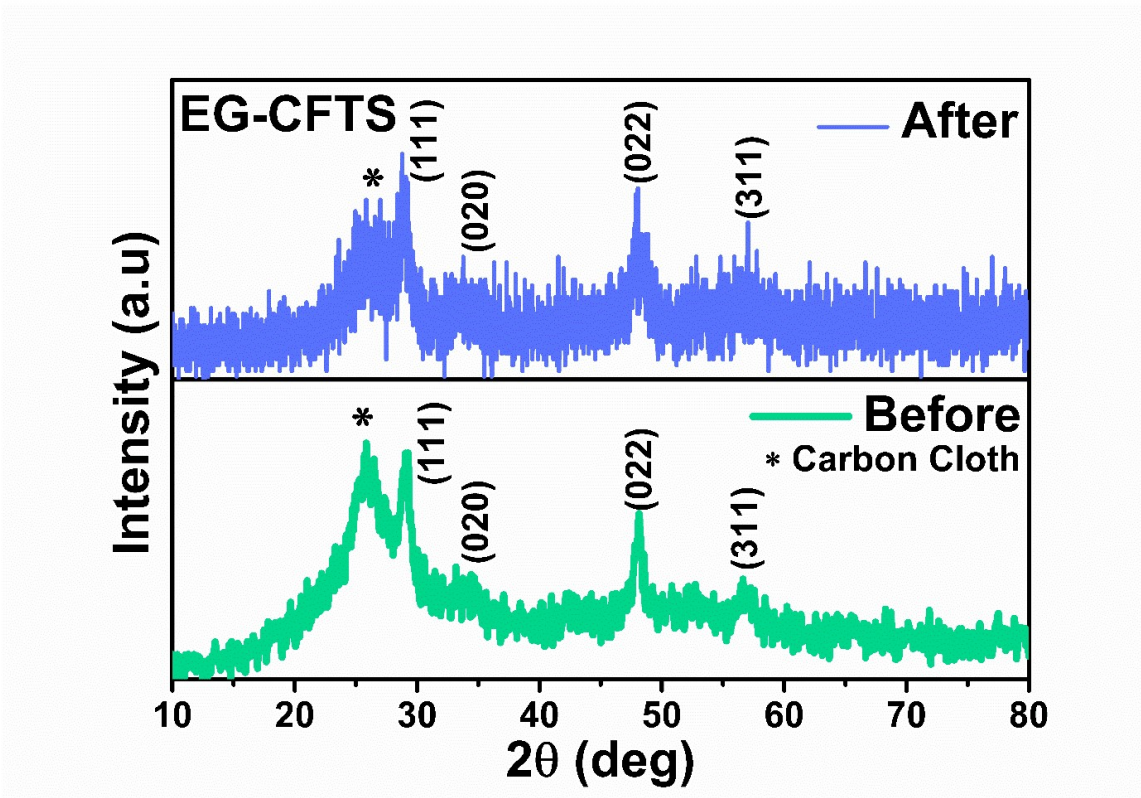


**Fig. S4** XRD spectra before and after electrochemical tests for EG-CFTS samples.

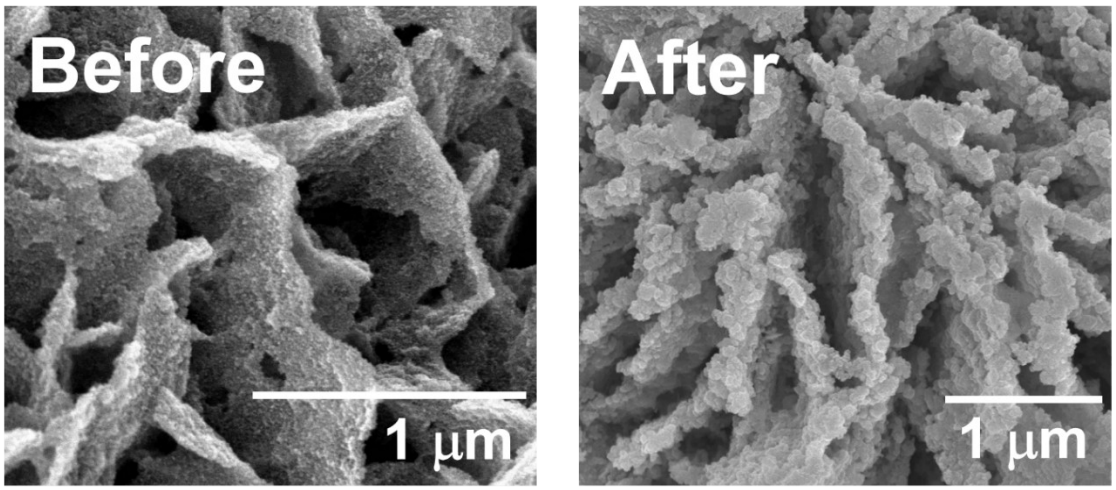


**Fig. S5** SEM images for EG-CFTS samples before and after electrochemical tests.

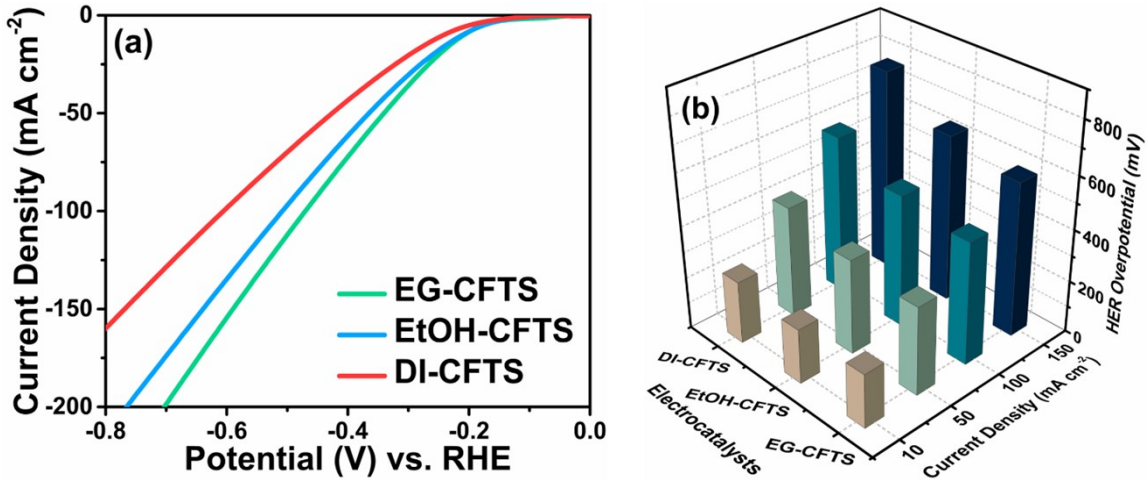


**Fig. S6** a) Linear sweep voltammetry (LSV) analysis and b). Comparison of current density and their corresponding HER overpotentials for the prepared CFTS electrocatalysts.

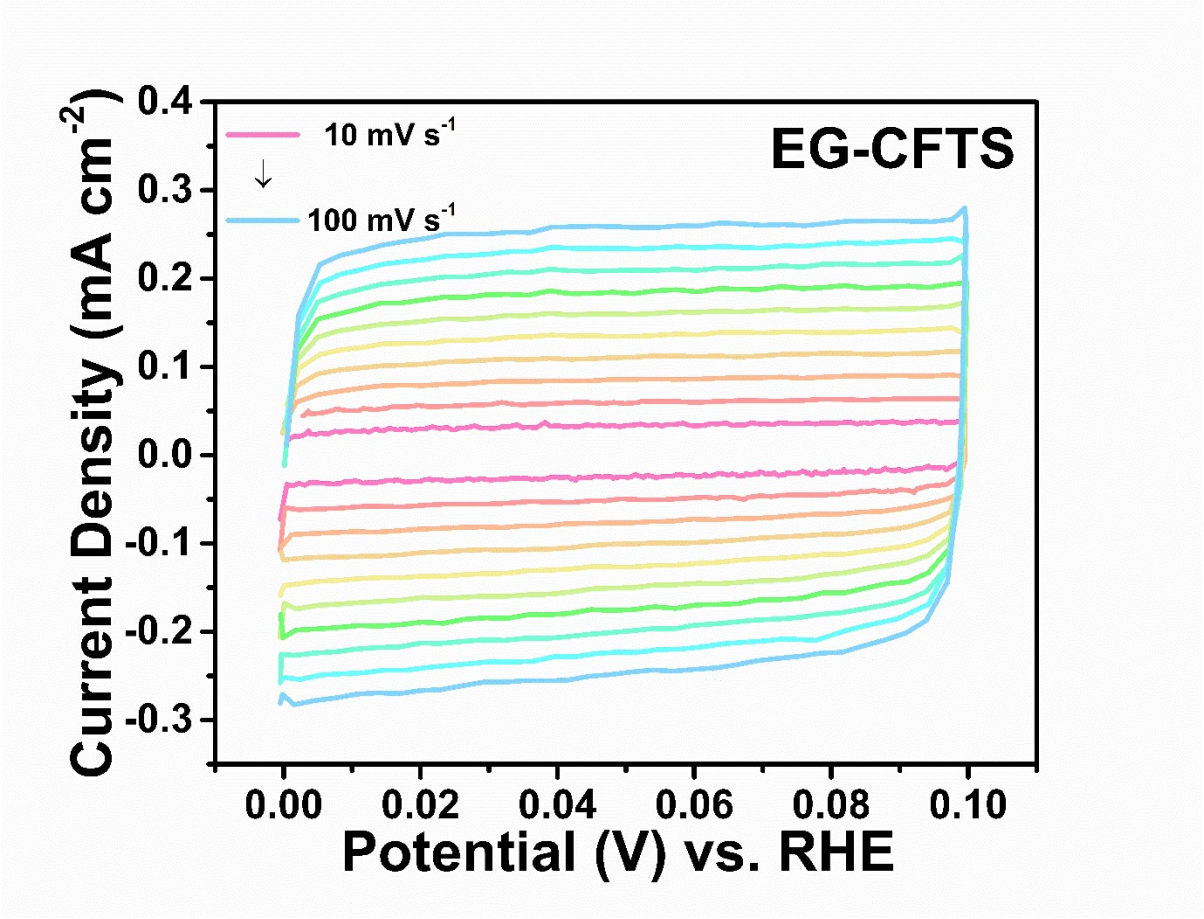


**Fig. S7** Cyclic Voltammograms of EG-CFTS electrocatalyst in the non-faradaic region at the scan rates from 10 to 100 mV $s^{-1}$.

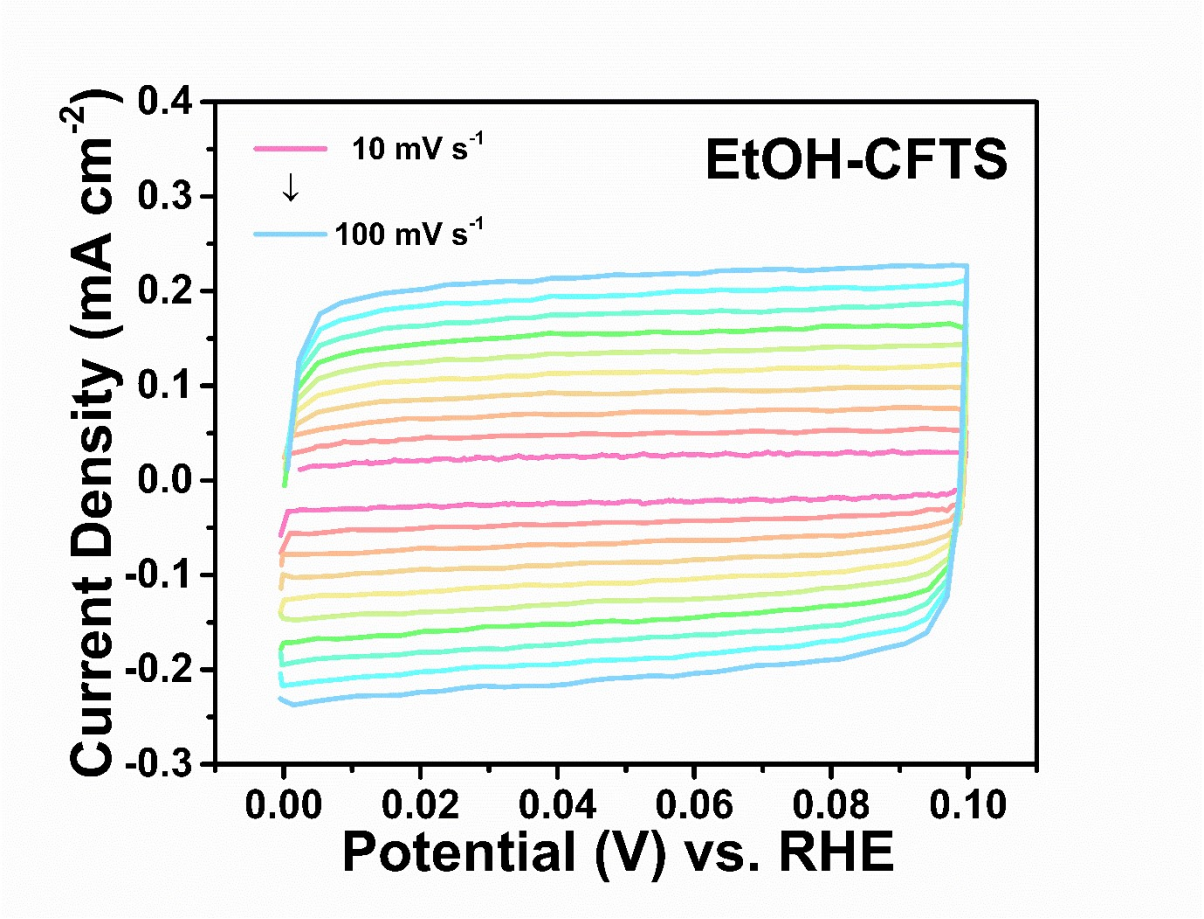


**Fig. S8** Cyclic Voltammograms of EtoOH-CFTS electrocatalyst in the non-faradaic region at the scan rates from 10 to 100 mV $s^{-1}$.

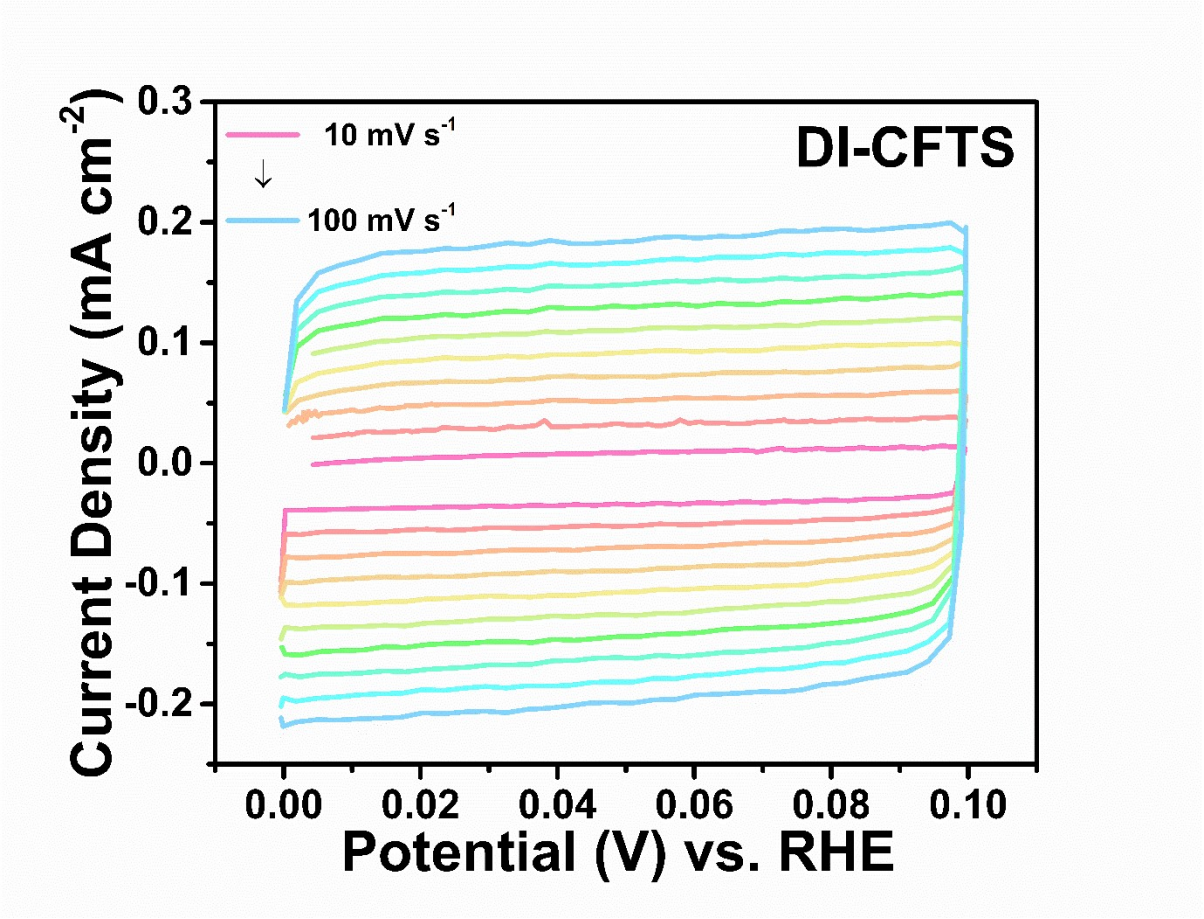


**Fig. S9** Cyclic Voltammograms of DI-CFTS electrocatalyst in the non-faradaic region at the scan rates from 10 to 100 mV $s^{-1}$.

**Table S1** EIS spectra fitting parameters.

| Electrocatalysts | R1 (Ω) | R2 (Ω) | S4 ($\Omega.s^{-1/2}$) |
|---|---|---|---|
| **EG-CFTS** | 1.169 | 0.384 | 364.5 |
| **EtOH-CFTS** | 1.322 | 0.413 | 377.7 |
| **DI-CFTS** | 1.317 | 0.496 | 622.1 |

**Table S2** Comparison of previously reported Cu-based electrocatalysts and their AOR performances.

| Catalyst | AOR Onset potential (V) | Electrolyte/ Solution | Potential | Current density (mA/cm$^2$) | Area of electrode (cm$^2$) | Ref. |
|---|---|---|---|---|---|---|
| **EG-CFTS** | **1.38 V vs. RHE** | **1 M KOH + 0.5 M $NH_4OH$** | **1.6 V vs. RHE** | **152.4 mA cm$^{-2}$** | **1 x 1** | **This work** |
| **EtOH-CFTS** | **1.42 V vs. RHE** | **1 M KOH + 0.5 M $NH_4OH$** | **1.6 V vs. RHE** | **96.1 mA cm$^{-2}$** | **1 x 1** | **This work** |
| **DI-CFTS** | **1.51 V vs. RHE** | **1 M KOH + 0.5 M $NH_4OH$** | **1.6 V vs. RHE** | **57.3 mA cm$^{-2}$** | **1 x 1** | **This work** |
| NiCu/CP | 0.47 V vs. Ag/AgCl | 0.5 M NaOH + 55 mM $NH_4Cl$ | 0.7 V vs. Ag/AgCl | 52 mA cm$^{-2}$ | 2 | S1 |
| NiCu layered hydroxides (LHs) | ~0.43 V vs. Ag/AgCl | 0.5 M NaOH + 55 mM $NH_4Cl$ | 0.55 V vs. Ag/AgCl | 35 mA cm$^{-2}$ | 1 x 3 | S2 |
| Defect engineered CuO | 0.29 V vs. Hg/HgO | 1 M KOH + 1 M $NH_3$ | 0.6 V vs. Hg/HgO | 200 mA cm$^{-2}$ | 2 x 1 | S3 |
| Ni-$(OH)_2$-$Cu_2O$@CuO | 0.47 V vs Hg/HgO | 1 M KOH + 1 M $NH_3$ | 0.6 V vs. Hg/HgO | 60 mA cm$^{-2}$ | 3 x 5 | S4 |
| NiCu/C/CP | 0.39 V vs. Hg/HgO | 1 M KOH + 0.5 M $NH_3$ | 0.65 V vs. Hg/HgO | 110.4 mA cm$^{-2}$ | 1 x 1 | S5 |
| $CuSn(OH)_6$ | 0.85 V vs. Hg/HgO | 0.5 M $K_2SO_4$ + 10 mM $NH_3$ | 1.23 V vs. Hg/HgO | 0.85 mA cm$^{-2}$ | 1 x 0.5 | S6 |
| PtIrCu HCOND | 0.35 V vs. RHE | 0.1 M $NH_3$ + 1 M KOH | 0.65 V vs. RHE | 31.8 A $g_{PtIr}^{-1}$ | 0.196 (Glassy carbon) | S7 |
| $La_{0.5}Sr_{1.5}Ni_{0.9}Cu_{0.1}O_{-\delta}$-Ar | ~0.4 V vs. Ag/AgCl | 0.5 M KOH + 55 mM $NH_4Cl$ | 0.53 V vs. Ag/AgCl | 13.4 mA cm$^{-2}$ | -- | S8 |
| LNCO55-Ar | 0.42 V vs. Ag/AgCl | 0.5 M KOH + 55 mM $NH_4Cl$ | 0.5 V vs. Ag/AgCl | 14.4 mA cm$^{-2}$ | 2.5 x 2.5 | S9 |
| NiCu/$MnO_2$ | 0.53 V vs. Hg/HgO | 0.5 M NaOH + 55 mM $NH_4Cl$ | 0.6 V vs. Hg/HgO | 8.2 mA cm$^{-2}$ | 1 x 1 | S10 |

## References

[S1] W. Xu, D. Du, R. Lan, J. Humphreys, D. N. Miller, M. Walker, Z. Wu, J. T. S. Irvine and S. Tao, Applied Catalysis B: Environmental, 2018, 237, 1101-1109.

[S2] W. Xu, R. Lan, D. Du, J. Humphreys, M. Walker, Z. Wu, H. Wang and S. Tao, Applied Catalysis B: Environmental, 2017, 218, 470-479.

[S3] J. Huang, Z. Chen, J. Cai, Y. Jin, T. Wang and Jianhui Wang, Nano Res., 2022, **15**, 5987–5994.

[S4] J. Huang, J. Cai, and J. Wang, ACS Appl. Energy Mater., 2020, **3**, 4108–4113.

[S5] H. Zhang, Y. Wang, Z. Wu, D. Y. C. Leung, Energy Procedia, 2017, **142**, 1539-1544.

[S6] J. Hou, Y. Cheng, H. Pan and P. Kang, ChemElectroChem 2022, 9, e202101301.

[S7] X. Lin, X. Zhang, Z. Wang, X. Zhu, J. Zhu, P. Chen, T. Lyu, C. Li, Z. Q. Tian, P. K. Shen, Journal of Colloid and Interface Science, 2021, 601, 1–11.

[S8] M. Zhang, P. Zou, G. Jeerh, B. Sun, M. Walker and S. Tao, Adv. Funct. Mater. 2022, 32, 2204881.

[S9] M. Zhang, H. Li, X. Duan, P. Zou, G. Jeerh, B. Sun, S. Chen, J. Humphreys, M. Walker, K. Xie and S. Tao, Adv. Sci. 2021, 8, 2101299

[S10] K. Nagita, Y. Yuhara, K. Fujii, Y. Katayama and M. Nakayama, ACS Appl. Mater. Interfaces 2021, 13, 28098–28107.